

Supporting Information

High performance All-Solid-State Li-Se Batteries induced by sulfide electrolyte

*Xiaona Li⁺, Jianwen Liang⁺, Xia Li, Changhong Wang, Jing Luo, Ruying Li, and Xueliang Sun**

Methods

Preparation of the Se-Li₃PS₄-C cathode composite: The commercial Se powder (99.5%, Sigma-Aldrich) was mixed with Li₃PS₄ (99.95%, MSE supplies, LLC) and acetylene black (AB) at a weight ratio of 40:40:20 by ball milling for 4 h.

Synthesis of Li-Sn anode: 2 g of Li metal foil were heated and melted at 250 °C in stainless steel pan inside glovebox. After melting, the surface oxide layer was removed carefully by stainless steel tweezers to obtain a bright and beaded molten lithium. Then, 6 g of Sn powder (99.8%, Aldrich) were added and the temperature of the stainless steel pan was still kept at 250 °C for 10 minute. When the temperature turn down, a soft alloy particle with white color could be achieved. The resulting alloy particle were press under 100 MPa to form the Li-Sn anode foils. Both of Li and Li₂₂Sn₅ were detected by XRD measurement in the obtained Li-Sn anode foils (Figure S10).

Electrochemical measurements: All-solid-state cells (Se/Li₃PS₄/Li or Se/Li₃PS₄/Li Li-Sn) were assembled to examine the electrochemical performance of Se. The commercial Li₃PS₄ powders were used as a solid electrolyte separator. Lithium or Li-Sn alloy foil was used as the negative electrode.

The all-solid-state cells were fabricated as follows: 100 mg of the Li₃PS₄ was pressed successively under 240 MPa to form solid electrolyte layer. The cathode composite powder was uniformly spread onto the surface of the Li₃PS₄ electrolyte and pressed under 360 MPa. Li or Li-Sn alloy foil was subsequently pressed onto the other side of the Li₃PS₄ layer under 120 MPa. The mass loading of cathode is about 7.6 mg cm⁻², corresponding to a Se loading of 3 mg cm⁻². The three-layered pellet was sandwiched between two stainless-steel rods as current collectors for both positive and negative electrodes. All the processes were performed in an Ar-filled glove box.

All-solid-state cells were tested at different current densities by using a multichannel battery tester (LAND CT-2001A, Wuhan Rambo Testing Equipment Co., Ltd.). Rate capability and cycling stability were tested using an operating voltage window of 1.0-3.0 V (vs Li/Li⁺). After

charging at a constant current, the cells were further charged at a constant voltage of 3.0 V until the current dropped to 10% of the constant current. All electrochemical tests were performed at room temperature unless otherwise noted. The galvanostatic intermittent titration technique (GITT) measurements were performed using LAND battery testing station, by applying a current density of 20 mA g⁻¹ for 1 h followed by a 4-h relaxation. Cyclic voltammograms (CVs) were performed on a versatile multichannel potentiostation 3/Z (VMP3) under a scanning rate of 0.05 mV s⁻¹ between 1.0 to 3.0 V (vs. Li/Li⁺). Electrochemical Impedance Spectroscopy (EIS) measurements for all-solid-state cells were also conducted with VMP3 at different discharge/charge states with an amplitude of 10 mV and frequencies ranging from 0.1 Hz to 7 MHz.

Characterizations: Hitachi S-4800 field-emission scanning electron microscope (FE-SEM) equipped with energy dispersive spectroscopy (EDS) was used to characterize the morphologies of the samples. X-ray diffraction (XRD) measurements were performed on Bruker AXS D8 Advance with Cu K α radiation ($\lambda = 1.54178 \text{ \AA}$). Raman spectra were measured with a HORIBA Scientific LabRAM HR Raman spectrometer operated with an incident laser beam at 532.03 nm. For X-ray photoelectron spectroscopy (XPS) analysis, the electrodes at different charge or discharge state were disassembled and transferred to XPS (Krotos AXIS Ultra Spectrometer) system using an Ar-filled glove box to avoid exposure to air or moisture.

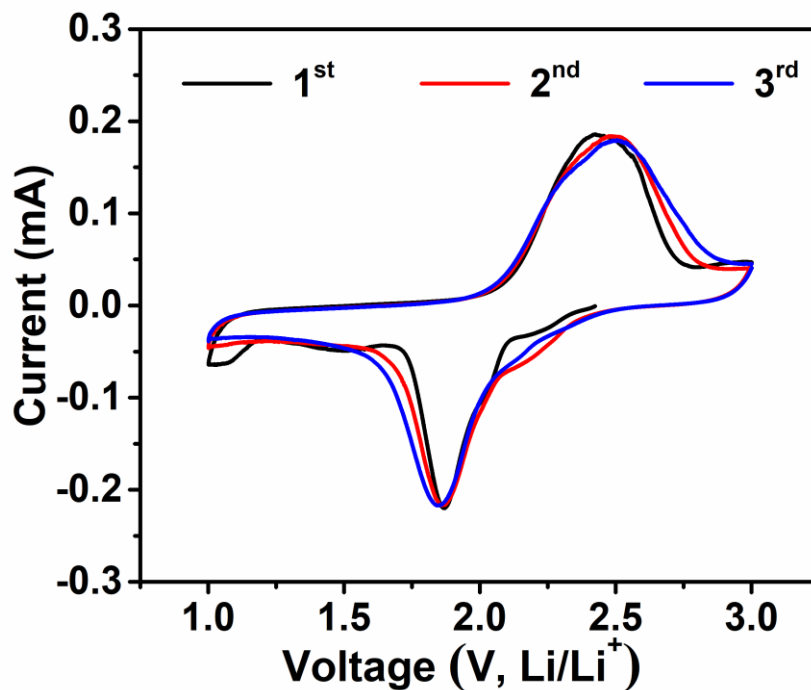


Figure S1. Cyclic voltammogram of Se cathode in all-solid-state cell at 60 °C in the potential range from 1.0 to 3.0 V at 0.05 mV s⁻¹.

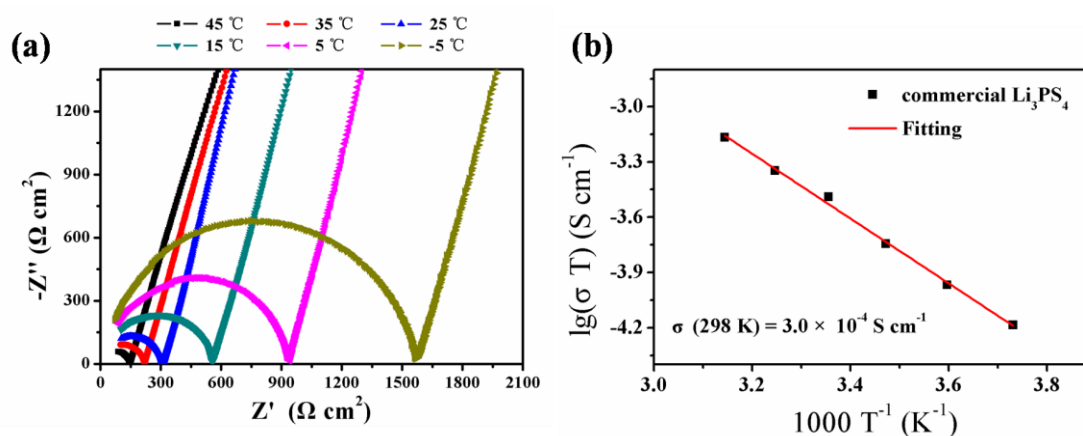


Figure S2. (a) Impedance plots of commercial Li₃PS₄ under different temperatures (-5, 5, 15, 25, 35 and 45 °C). (b) Arrhenius plots of ionic conductivity for commercial Li₃PS₄.

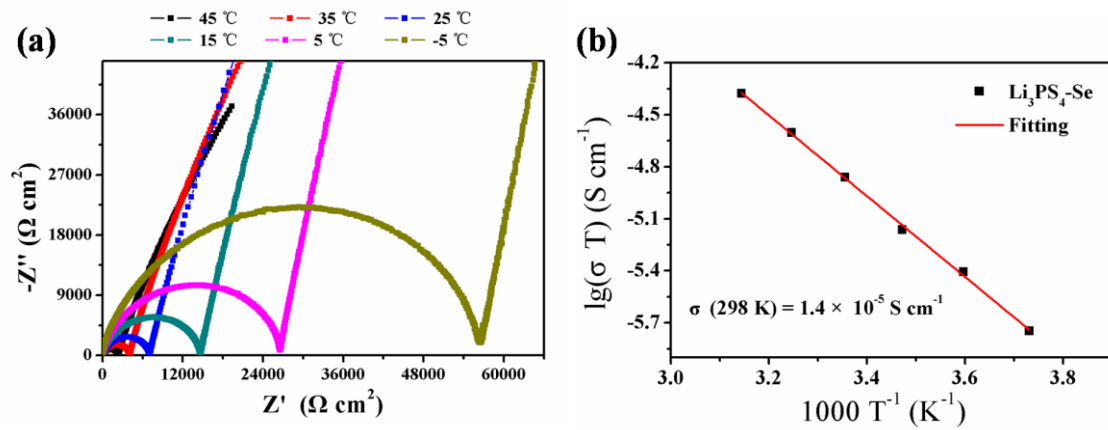


Figure S3. (a) Impedance plots of $\text{Li}_3\text{PS}_4\text{-Se}$ composite under different temperatures (-5, 5, 15, 25, 35 and 45°C). (b) Arrhenius plots of ionic conductivity for $\text{Li}_3\text{PS}_4\text{-Se}$ composite.

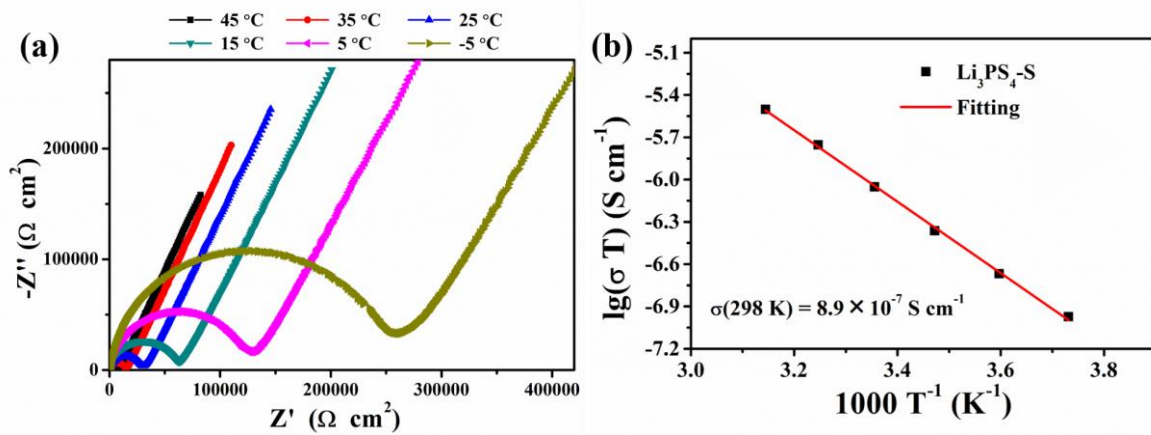


Figure S4. (a) Impedance plots of $\text{Li}_3\text{PS}_4\text{-S}$ composite under different temperatures (-5, 5, 15, 25, 35 and 45°C). (b) Arrhenius plots of ionic conductivity for $\text{Li}_3\text{PS}_4\text{-S}$ composite.

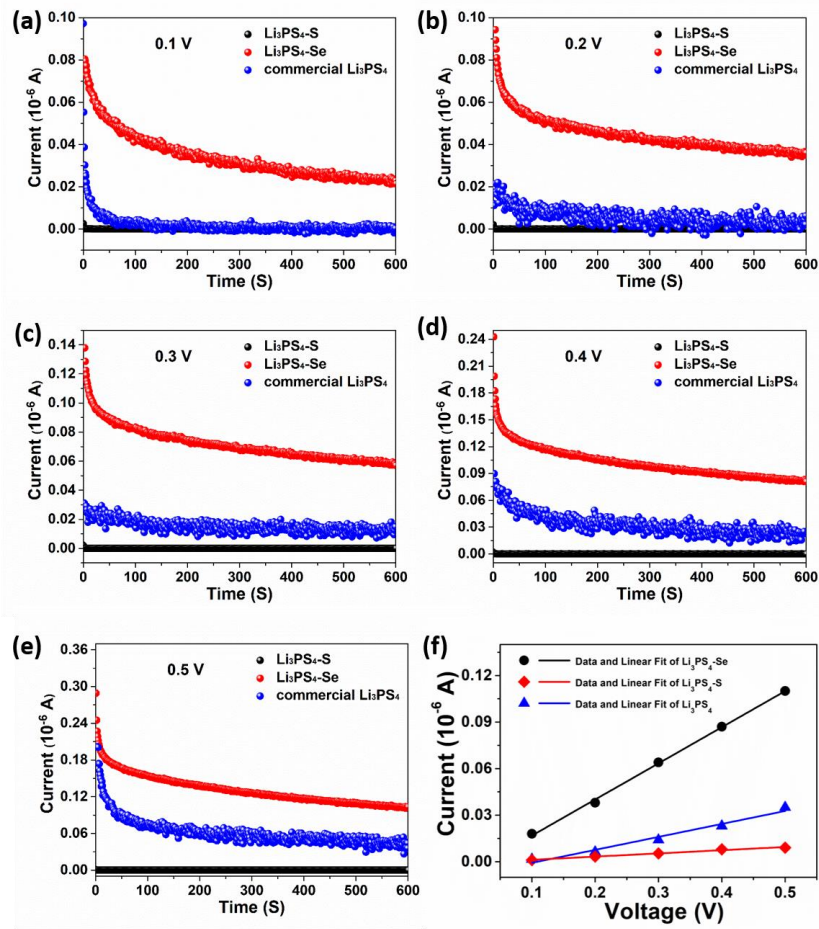


Figure S5. (a-e) DC polarization curves of $\text{Li}_3\text{PS}_4\text{-Se}$, $\text{Li}_3\text{PS}_4\text{-S}$ and Li_3PS_4 using symmetric cells at different voltages. (f) Stable current response of $\text{Li}_3\text{PS}_4\text{-Se}$, $\text{Li}_3\text{PS}_4\text{-S}$ and Li_3PS_4 using symmetric cells at different voltages.

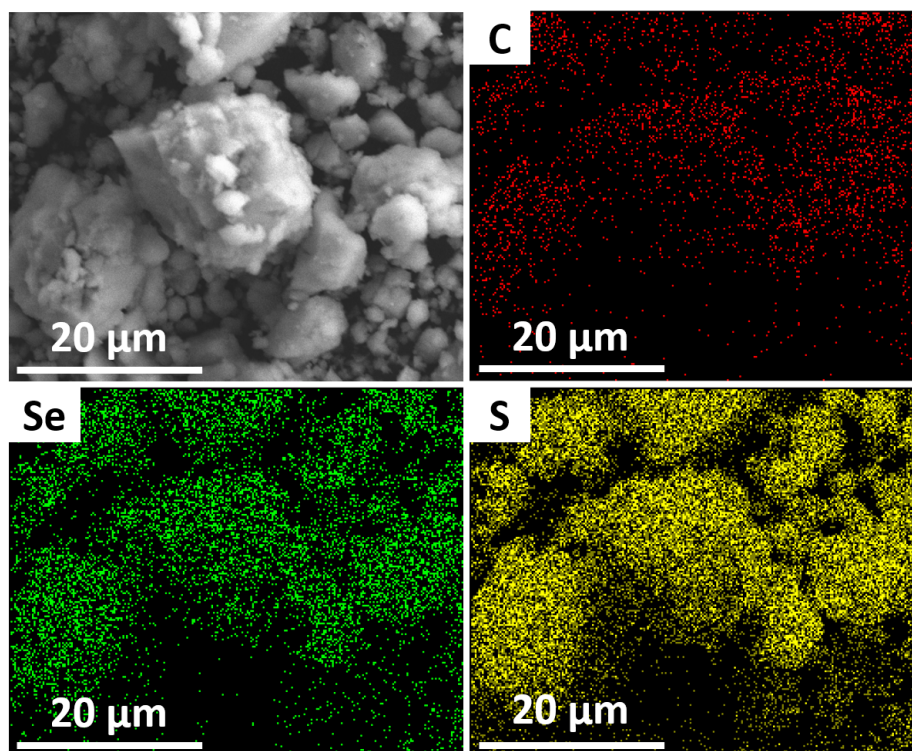


Figure S6. SEM and EDX mapping of Se-Li₃PS₄-C cathode composite after ball milling process.

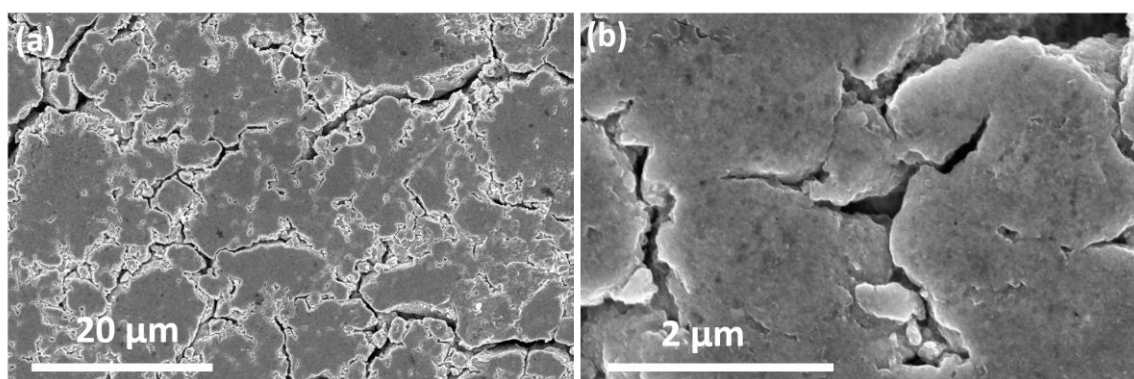


Figure S7. SEM images (top view, cathode side) of Se-Li₃PS₄-C/Li₃PS₄ pellet pressed at 360 MPa.

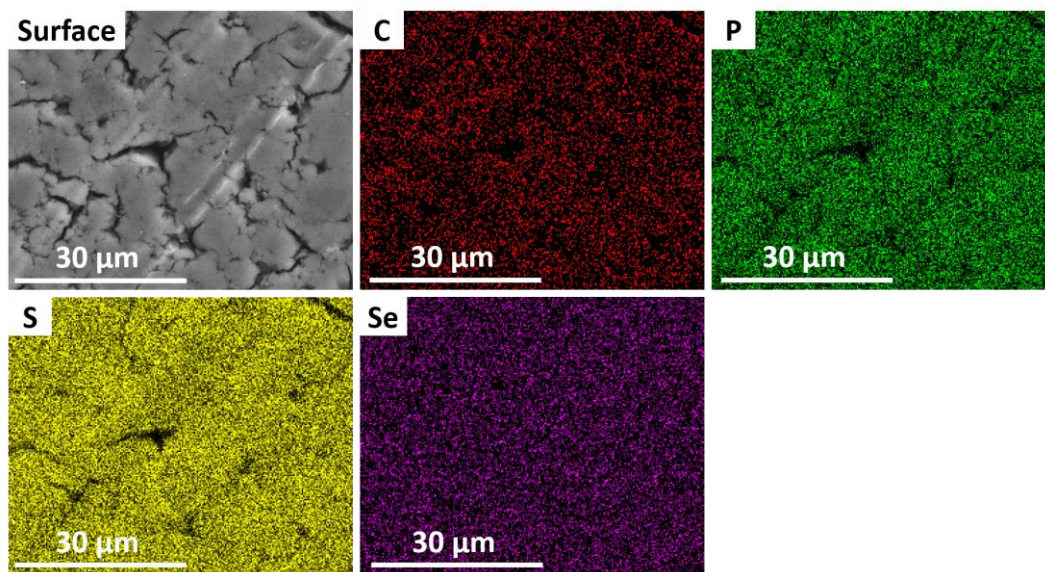


Figure S8. SEM image (top view, cathode side) of Se-Li₃PS₄-C/Li₃PS₄ pellet pressed at 360 MPa and corresponding EDX mapping of C, P, S and Se.

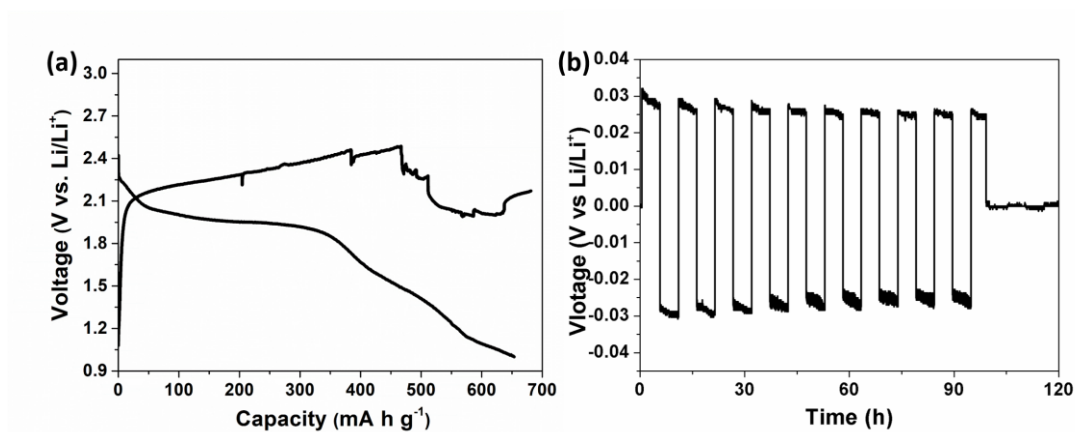


Figure S9. (a) Charge/discharge curves of an all-solid-state Se/Li₃PS₄/Li cell using a lithium foil at 50 mA g⁻¹ at 25 °C. (b) Lithium cyclability in a symmetric Li/Li₃PS₄/Li cell. The cell was cycled at a current density of 0.05 mA cm⁻² at room temperature and 25 °C.

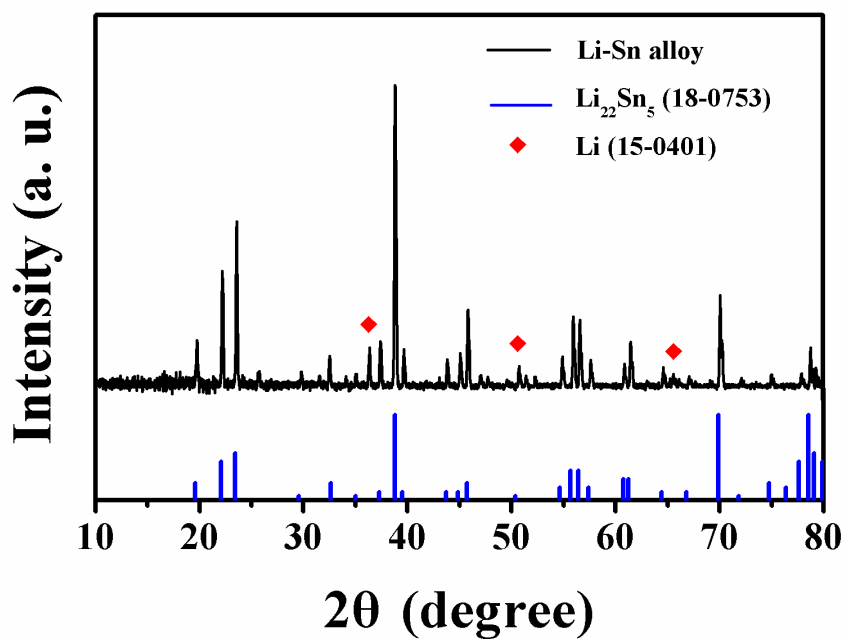


Figure S10. XRD pattern of the as-prepared Li-Sn alloy.

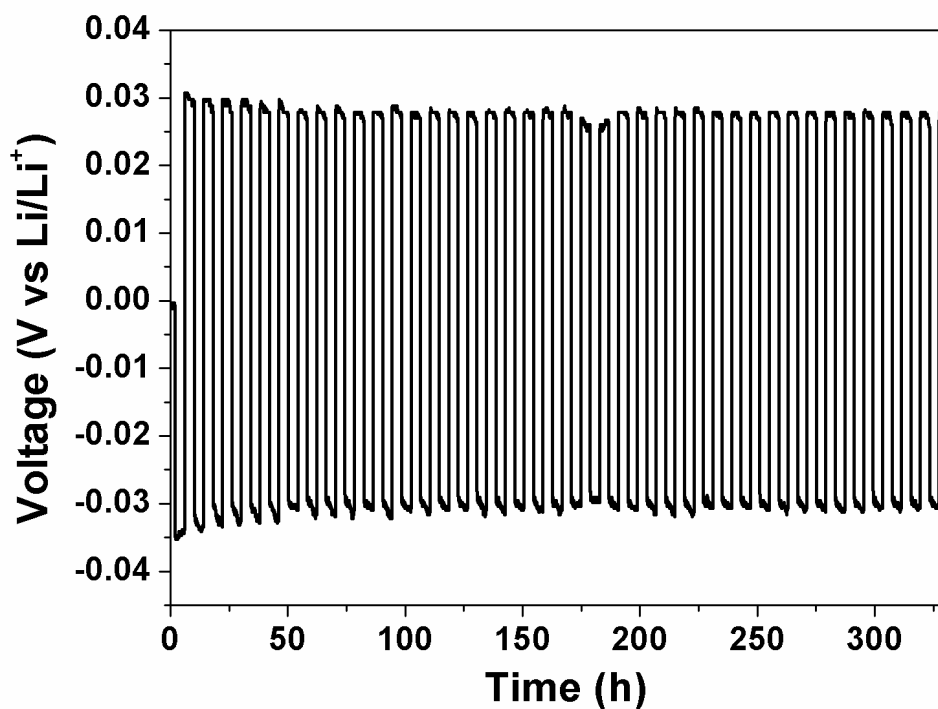


Figure S11. Lithium cyclability in a Li-Sn/Li₃PS₄/Li-Sn symmetric cell. The cell was cycled at a current density of 0.05 mA cm⁻² at room temperature.

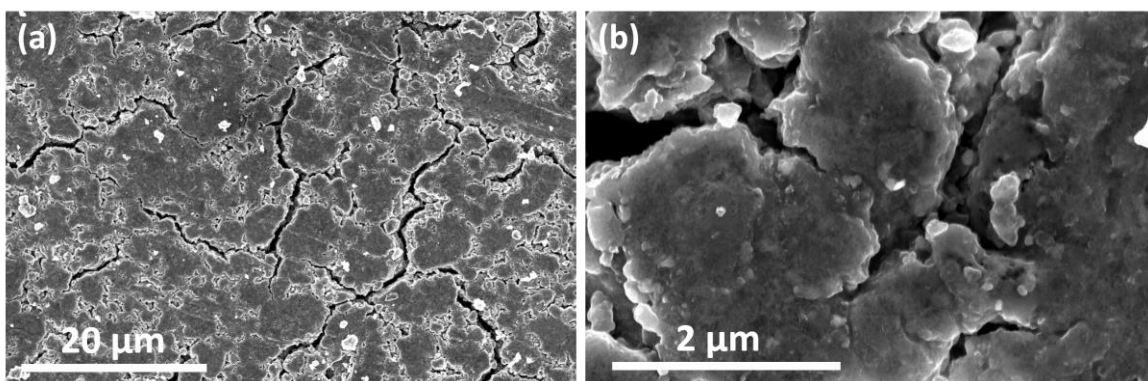


Figure S12. SEM images (top view, cathode side) of Se-Li₃PS₄-C/Li₃PS₄ pellet after 100 cycles.

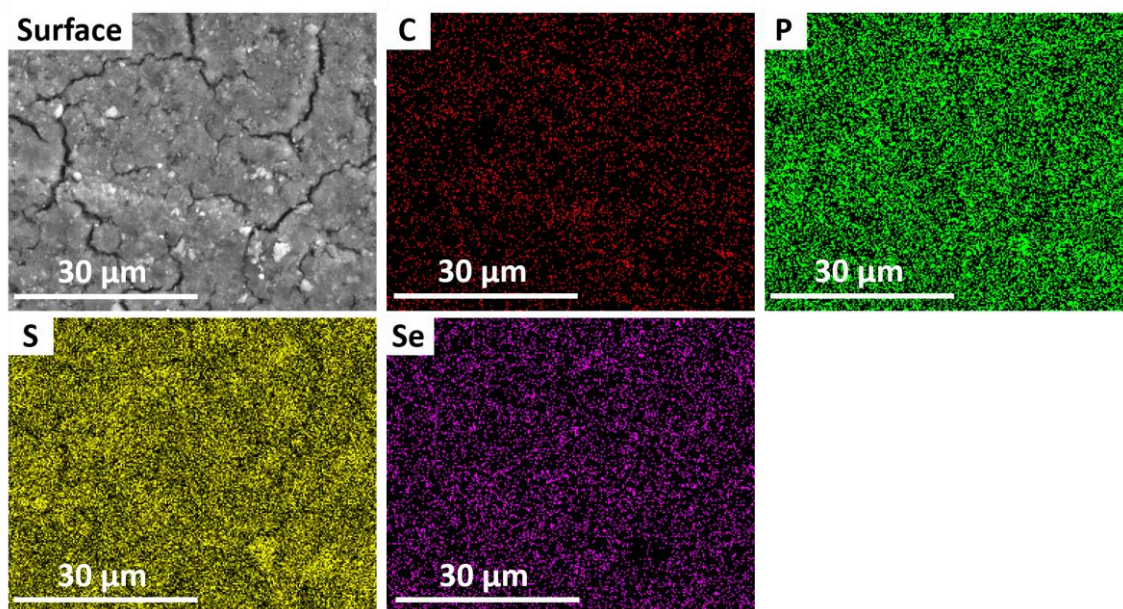


Figure S13. SEM image (top view, cathode side) of Se-Li₃PS₄-C/Li₃PS₄ pellet after 100 cycles and corresponding EDX mapping of C, P, S and Se.

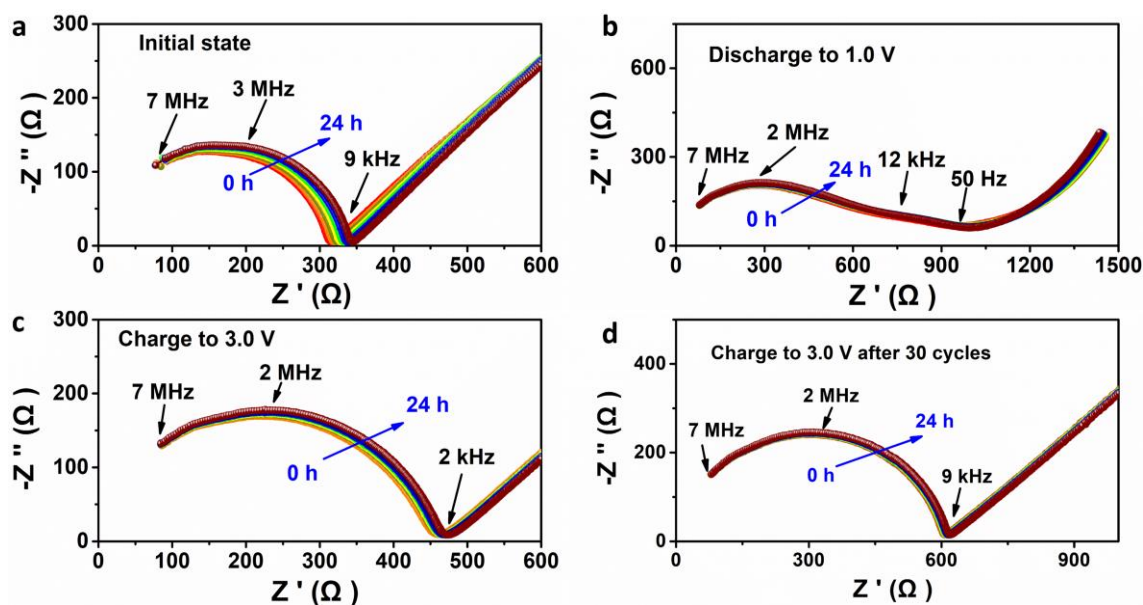


Figure S14. Nyquist plots of Se/Li₃PS₄/Li-Sn all-solid-state batteries at (a) initial state before discharge/charge, (b) first discharge to 1.0 V, (c) first charge to 3.0 V and (d) charge to 3.0 V after 30 cycles.

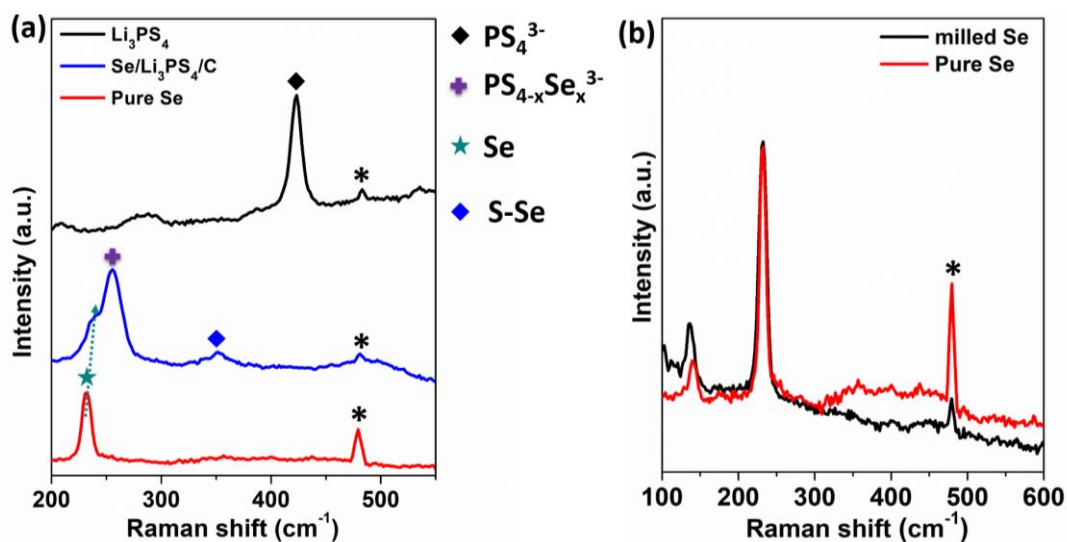


Figure S15. (a) Raman spectra of pure Se, commercial Li₃PS₄, Li₃PS₄/C and Se/Li₃PS₄/C. (b) Raman spectra of pure Se and Se after milling process. The signal marked as “*” in the spectra should be caused by fluorescent lamp during test.

It's noticed that the peak at 252 cm⁻¹ might also be assigned to Se with different allotropic form^[1]. Thus to make sure the assignment of this new peak after ball-milling process, the Raman spectra of commercial pure Se before and after ball-milling process were also

compared as shown in Figure S14b. It could be seen that the peaks didn't show obvious change, indicating no other selenium allotropic form emerged after ball-milling process.

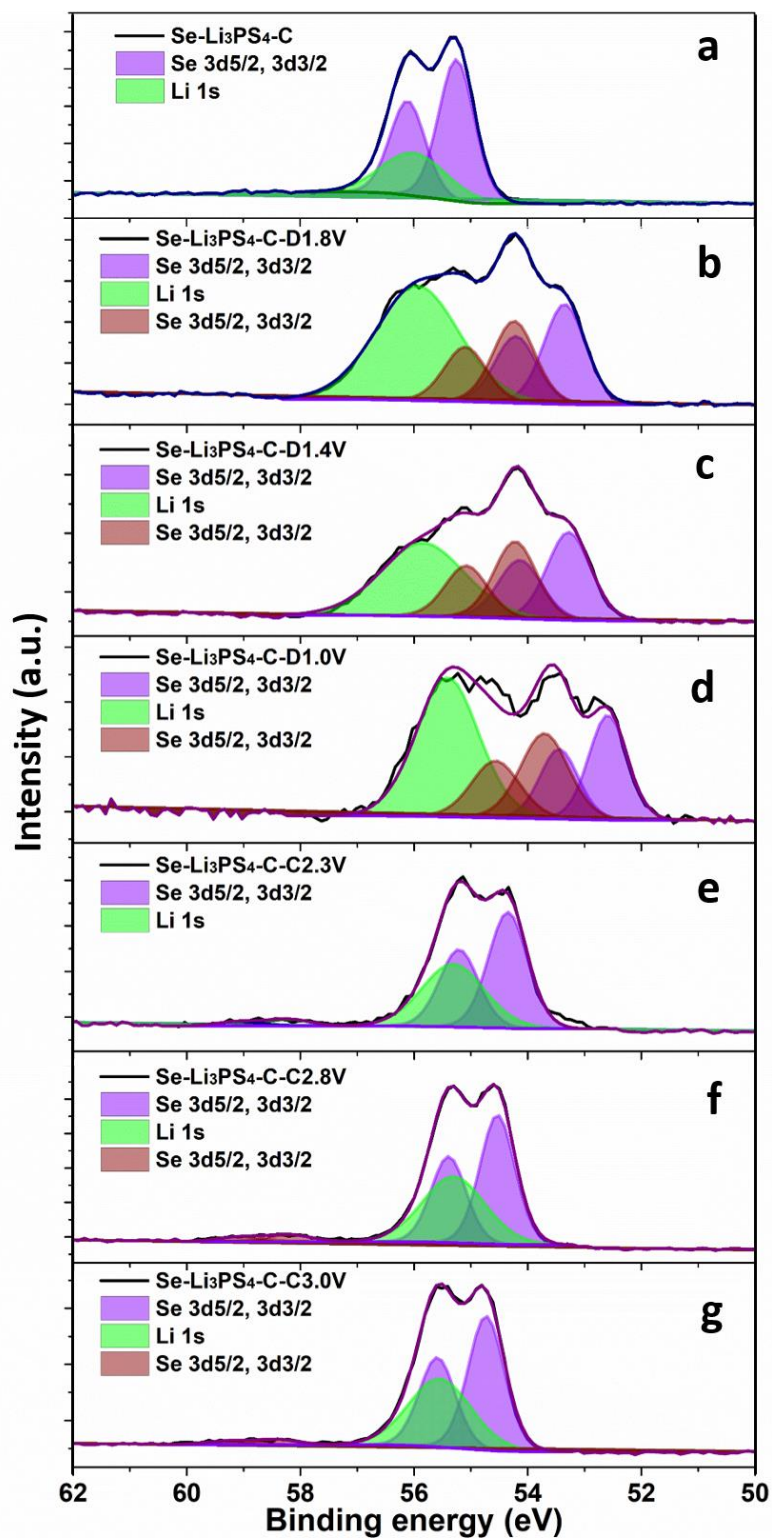


Figure S16. Se 3d and Li 1s XPS spectra of Se/Li₃PS₄/C cathode at different discharge/charge states. (a for fresh state, b for discharged at 1.8 V vs. Li/Li⁺, c for discharged at 1.4 Li/Li⁺, d

for discharge to 1.0 V Li/Li⁺, e for charged to 2.3 V Li/Li⁺, f for charged to 2.8 V Li/Li⁺, and g for charged to 3.0 V Li/Li⁺).

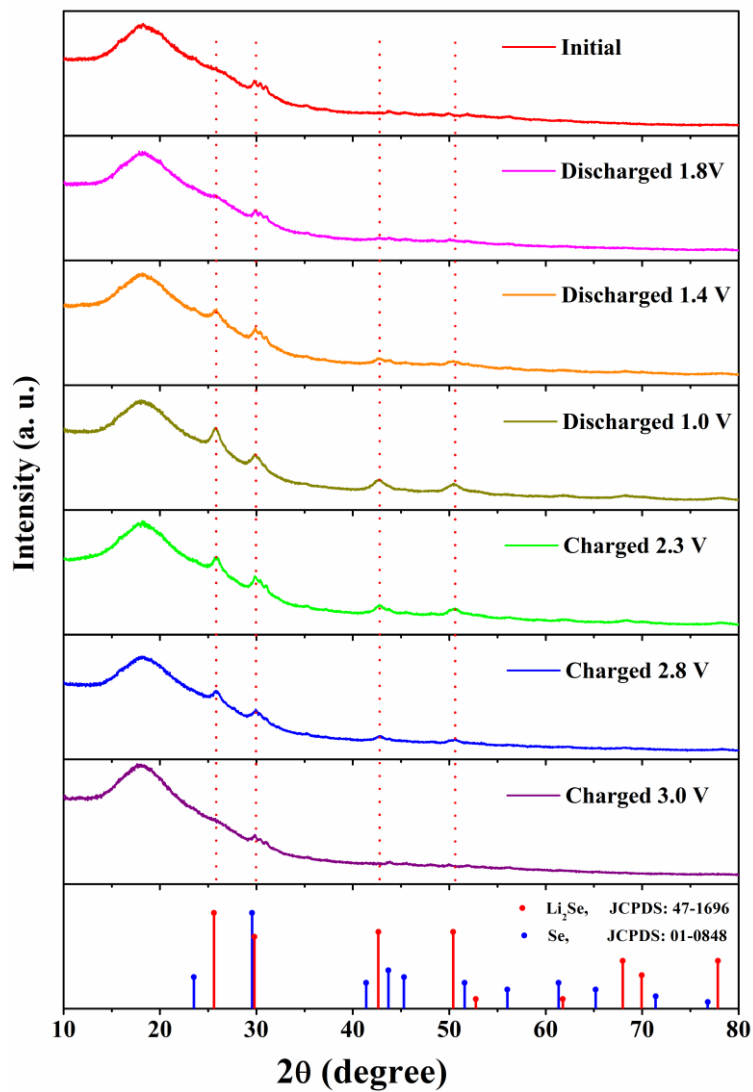


Figure S17. *EX-situ* XRD patterns of Se/Li₃PS₄/C cathode at different discharge/charge states.

[1] M. Steichen, P. Dale, *Electrochemistry Communications* **2011**, *13*, 865-868.